PROCEEDINGS OF SCIENCE

Multiwavelength view of OJ 287 during 2017-2020

Aditi Agarwal[a,*]

[a] *Raman Research Institute,*
C. V. Raman Avenue, Sadashivanagar, Bengaluru - 560 080, India

E-mail: aditiagarwal.phy@gmail.com

Based on the optical studies, the blazar OJ 287 has been proposed as a binary black hole system, thus making it an interesting source to study further. In this work, we analyzed the optical, UV, X-ray, and γ-ray data of the source spanning a period from 2017 – 2020. According to the observed variability in optical and X-rays, this period is divided into five segments, namely, A, B, C, D, and E. To understand the nature of temporal variability, we studied intraday variability and estimated fractional variability for above mentioned five states. Also, we modeled the multiwavelength spectral energy distribution (SED) to have a better understanding of simultaneous broadband emission. The blazar OJ 287 was found to be in a high state and displayed significant flux variability in optical, UV, and X-rays during the period in the study. In contrast, Fermi-LAT shows moderate flux variations during this time period. Finally, a single-zone synchrotron self-Compton (SSC) emission model is found to best explain the nature of the blazar OJ 287.

7th Heidelberg International Symposium on High-Energy Gamma-Ray Astronomy (Gamma2022)
4-8 July 2022
Barcelona, Spain

*Speaker

PoS(Gamma2022)179

1. Introduction

The blazar OJ 287 is a BL Lacertae, with a redshift of 0.306 [1]. Blazars display variability along the entire electromagnetic spectrum and on diverse timescales. Variability can be broadly divided into intraday variability (IDV) for changes on timescale minutes to hours [e.g. 2, 3]; those on a timescale of days to a few months are short-term variations (STVs); and changes over several months to years are long-term variations [LTV, e.g. 4]. Later two classes can have amplitude changes of up to 5 magnitudes.

[5] first detected the intraday variability in radio and optical bands for the blazar OJ 287. While [6] analyzed the short-term variability using observational data collected for 23 months and found a magnitude change of 0.7. Long-term studies of the source have shown repeated outbursts after every 11.65 years, which has been attributed to the binary black hole model ([7]). Long-term multi-frequency light curves of OJ 287 were obtained using Swift UVOT and XRT, where they did not find any clear correlation between optical-UV and X-ray frequencies during various states of the source.

According to the binary black hole model of [7], a huge flare was predicted in 1994, which was then observed by [8]. The impact of the secondary black hole on the accretion disk of the primary one could be the reason behind these flares. But according to this, one should observe two flares during each orbital cycle. [9] observed the second flare in November 1995, which was in accordance with the model. Later [10, 11] predicted the flares due to tides from the binary model in 2008 – 2010. [12] analyzed the γ-ray light curve of OJ 287 during this period and detected a variability timescale of fewer than 3.2 hours. This attributes the γ-ray emission to the jet corresponding to the black hole with a smaller mass. [13] studied the December 2015 – April 2016 flare and found a common emission region. Moreover, they associated the optical bump with the accretion disk of the primary black hole. They also found the γ-ray emission to be consistent with the inverse Compton scattering of photons from the line emission. To explain the X-ray and γ-ray outbursts of November 2015, [14] proposed a hadronic model where they use a binary supermassive black hole model. According to them, the initial trigger is due to the impact of the secondary black hole on the accretion disk of the primary black hole, thus creating an idealized spherical outflow containing cosmic rays and thermal ions. In their model, the cosmic ray protons interact with the thermal ions, and as a result, secondary leptons and photons are produced in proton-proton interactions. Recently, [15] detected a huge flare in X-ray, UV, and optical wavelengths from April to June 2020. They proposed that this outburst is jet-driven and is also consistent with the binary supermassive black hole model.

In this work, we studied the multiwavelength properties of OJ 287 from 2017 to 2020, including the outburst discussed by [15]. This period has been divided into five segments based on the variability timescale of optical and X-ray bands. We also performed the multi-frequency SED modeling using a time-dependent leptonic model, which includes synchrotron and synchrotron self-Compton (SSC) processes. The data used is discussed in section 2; results and discussion is given in section 3.

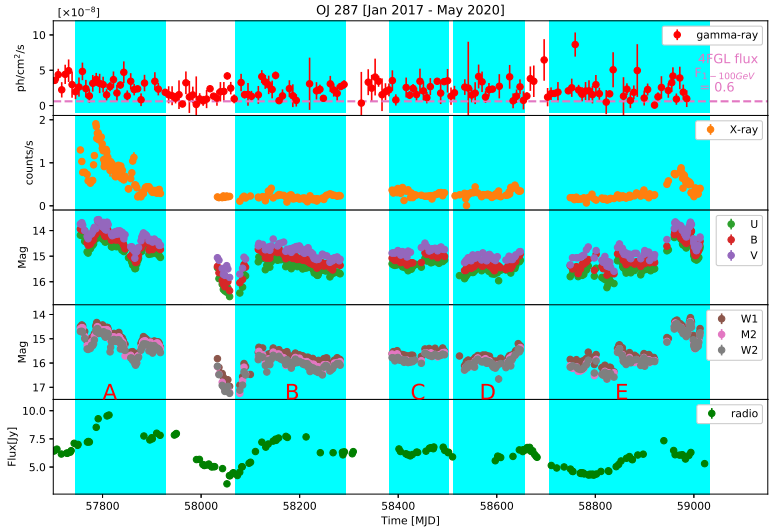

Figure 1: The broadband light curve of OJ 287 from 2017–2020. Panel 1 (top) shows the weekly binned γ-ray light curve for 0.1–300 GeV. Panels 2, 3, and 4 are the Swift-XRT and UVOT light curves. Panel 5 is the radio light curve from OVRO at 15 GHz. The light curve is divided into five states denoted A, B, C, D, and E, and their time range is represented by the color patches.

2. Observations and data analysis

For this work, we collected multi-wavelength data for the blazar OJ 287 from January 2017 to May 2020 using *Fermi*-LAT (gamma-rays), *Swift* telescope (X-rays, UV, optical), Owens Valley Radio Observatory (Radio). Moreover, we also observed the source using five different ground-based telescopes between Feb 2019 - Jan 2020. The details of these telescopes can be found in [16]. The data analysis methodology followed can be seen from [17]. More details on the data analysis software used for each telescope can be found in [18].

3. Results and Discussion

The multi-wavelength light curve from radio to gamma-ray extracted for the period January 2017 to May 2020 is shown in Figure 1. To characterize the long-term variability at various wavelengths, we used fractional variability, which is defined as:

$$F_{\rm var} = \sqrt{\frac{S^2 - err^2}{F^2}}, \tag{1}$$

where F denotes the mean flux, S^2 and err^2 are the variance and the mean square error in the flux, respectively. The flux doubling/halving time is also estimated for all bands [19]. We found the source to be the most variable in segment E, with the highest variability amplitude in all wavebands and the shortest (fastest) variability time (1 day). The values of variability amplitude vary from 50% to 60% among all frequencies.

We also studied the Intra-day Variability (IDV) using the C-criterion, and the F test [17]. We marked an LC to be variable only when both tests reject the null hypothesis at a 99.5% confidence level. Our total monitoring coverage contains 13 intraday LCs, from which we found only 1 variable LC (April 07, 2019). The relatively short span of 2 – 4 hours of observation time reduces the chances of detecting genuine variability. We found the brightest state reached by the source was on January 03, 2020, with R ∼ 14.38 mag, fainter than its brightest state in 2015 by ∼ 1.4 mags, while the faintest state attained by the source was on December 18, 2019, with R band mag of 15.15, approximately 2.15 mag fainter than its brightest state during the 2015 – 2016 outburst.

We have also produced the gamma-ray spectra for various states of the source using *likeSED.py*[1]. The details about the models are discussed in [20]. The isotropic γ-ray luminosity corresponding to each spectral model is estimated for all the segments and is estimated to be of the order 10^{47} – 10^{48} erg/s. The gamma-ray spectrum and model fitting are shown in Figure 2, and corresponding model parameters are presented in Table 1. Considering the PL spectral model, the spectral state of the source changes from segment A to Segment B, C, and D from harder (Γ = 1.90±0.06) to softer (Γ = 2.27±0.08)) and again it becomes harder from segment D (Γ = 2.35±0.10) to segment E (Γ = 2.21±0.06).

We performed *Likelihood* analysis which returns the TS (test statistics; [21]) corresponding to each model and is used to decide which model gives the best fit to the spectral data points. The TS_{curve} reveals the presence of curvature or a break in the spectrum, which could be caused by the absorption of high energy photons (> 20 GeV; [22]) by the broad-line region (BLR), assuming the emitting region is located within the BLR.

We generated multiwavelength spectral energy distribution (MWSED) for all the observations in different states. We used a publicly available time-dependent code, GAMERA[2] to model these SEDs. As discussed above, the blazar OJ 287 is variable in all passbands with a variability timescale of ∼ 1 day. Thus we modeled the MWSEDs with only synchrotron and SSC processes within a single emission zone. An example of MWSED modeling is depicted in Figure 2, and corresponding best-fit parameters are listed in Table 1. More details can be found in [18]. Considering 1 day variability time in γ-rays, we found the size of the emission region to be r∼4.0×10^{16}cm (using r∼ c t_{var} δ/(1+z), where δ = 20).

We have also calculated the total power of the jet and of the individual jet components (leptons, magnetic field, protons). The Eddington luminosity for the primary BH is found to be L_{Edd} = 4πGmm$_p$c/σ_T, where m is the mass of the primary BH, m$_p$ is the proton mass, and σ_T is the Thompson scattering cross-section. The primary BH mass was estimated [13] by modeling the NIR–optical spectrum with an accretion disk as ∼1.8×10^{10}M$_\odot$. During the flaring states A and E, we found that the total jet power was 1.5 times higher than that for B and C. We also found that more luminosity in highly energetic electrons is required to produce the multiwavelength emission during A and E. The non-thermal flares during states A and E might have resulted from disk impact in November-December 2015 [23] and July-September 2019 [24], respectively.

The model of [11] predicted a major increase in accretion rate at the beginning of January 2020. However, the non-thermal flares happened during April-June 2020, nearly 4 months after

[1]https://fermi.gsfc.nasa.gov/ssc/data/analysis/user/

[2]http://libgamera.github.io/GAMERA/docs/main_page.html

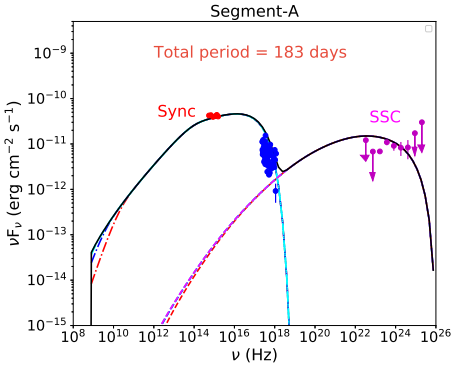

Figure 2: The Multiwavelength spectral energy distribution. The dot-dashed and dashed lines in different colors in the synchrotron and SSC peaks are the time evolution of the model. The optical–UV, X-ray, and γ-ray data points are shown in red, blue, and magenta, respectively.

their predicted time. The physical explanation for this delay requires a better understanding of the disk–jet connection as discussed by [15].

Between 2017 - 2020, the source did not attain any bright flaring state, but various high flux states were reported in numerous ATels in optical, UV, and X-rays. Based on these high states, we divided the LC into A, B, C, D, and E. As can be seen from Figure 1) and also evident from the SED modeling, states A and E appear to be the brightest. In the disk impact model, thermal bremsstrahlung radiation can be explained by the outbursts in optical–UV frequency owing to the impact of the secondary black hole on the accretion disk of the primary black hole [25]. The disk impact leads to a time-delayed increase in accretion rate and hence jet activity, which then triggers after-flare effects. States A and E of our work can be explained with this model, whereas a model which requires low jet power will be able to explain states B, C, and D.

[15] found strong x-ray, optical, and UV flares from their study of large X-ray data observed from 2015 to 2020. They found a steep power-law spectrum at the peak of the X-ray flare with an index of 2.8. This hints towards the synchrotron origin of X-ray emission. Thus as suggested by [15], emission could be attributed to jet, which is also consistent with the binary black hole model. We also modeled different states of source considered in our study considering the emission produced from the jet. The blazar OJ 287 has been found to exhibit different behaviors at various epochs and at different frequencies, thus making the source even more interesting for further studies.

References

[1] J.R. Dickel, K.S. Yang, G.C. McVittie and J. Swenson, G. W., *A survey of the sky at 610.5 MHz. II. The region between declinations +15 and +22 degrees.*, **72** (1967) 757.

[2] S.J. Wagner and A. Witzel, *Intraday Variability In Quasars and BL Lac Objects*, **33** (1995) 163.

[3] T.A. Rector and E.S. Perlman, *A Search for Intraday Variability in the Blazar PKS 2005-489*, **126** (2003) 47 [astro-ph/0304059].

Table 1: Multiwavelength SED modeling results with the values of the best-fit parameters. The input injected electron distribution is LogParabola with reference energy 60 MeV. The Doppler factor and the Lorentz factor are fixed at 20.0 and 15.5, respectively.

High state	Parameters	Symbols	Values	Period
Segment-A				183 days
	Size of the emitting zone	r	2.6×10^{15} cm	
	Min Lorentz factor of emitting electrons	γ_{min}	350.0	
	Max Lorentz factor of emitting electrons	γ_{max}	2.8×10^{4}	
	Input injected electron spectrum (LP)	α	1.60	
	Curvature parameter of the PL spectrum	β	0.02	
	Magnetic field in emitting zone	B	5.9 G	
	Jet power in electrons	$P_{j,e}$	4.35×10^{44} erg/s	
	Jet power in magnetic field	$P_{j,B}$	2.12×10^{44} erg/s	
	Jet power in protons	$P_{j,P}$	3.39×10^{43} erg/s	
	Total jet power	P_{jet}	6.81×10^{44} erg/s	

[4] A. Agarwal, P. Mohan, A.C. Gupta, A. Mangalam, A.E. Volvach, M.F. Aller et al., *Core shift effect in blazars*, **469** (2017) 813 [1704.03229].

[5] E. Valtaoja, H. Lehto, P. Teerikorpi, T. Korhonen, M. Valtonen, H. Teräsranta et al., *A 15.7-min periodicity in OJ287*, **314** (1985) 148.

[6] D. Lorenzetti, E. Massaro, G.C. Perola and L. Spinoglio, *Short Time Scale Variability of the BL Lacertae Object OJ 287 in the Near-Infrared*, **71** (1989) 175.

[7] A. Sillanpaa, S. Haarala, M.J. Valtonen, B. Sundelius and G.G. Byrd, *OJ 287: Binary Pair of Supermassive Black Holes*, **325** (1988) 628.

[8] A. Sillanpaa, L.O. Takalo, T. Pursimo and H.J. Lehto, *Confirmation of the 12-year optical outburst cycle in blazar OJ 287.*, **305** (1996) L17.

[9] A. Sillanpaa, L.O. Takalo, T. Pursimo, K. Nilsson, P. Heinamaki, S. Katajainen et al., *Double-peak structure in the cyclic optical outbursts of blazar OJ 287.*, **315** (1996) L13.

[10] B. Sundelius, M. Wahde, H.J. Lehto and M.J. Valtonen, *Long-time Brightness Variations of 0J287 in the Binary Black Hole Model*, in *Blazar Continuum Variability*, H.R. Miller, J.R. Webb and J.C. Noble, eds., vol. 110 of *Astronomical Society of the Pacific Conference Series*, p. 99, Jan., 1996.

[11] B. Sundelius, M. Wahde, H.J. Lehto and M.J. Valtonen, *A Numerical Simulation of the Brightness Variations of OJ 287*, **484** (1997) 180.

[12] A. Neronov and I. Vovk, *Fast variability of γ-ray emission from supermassive black hole binary OJ 287*, **412** (2011) 1389 [1011.4020].

[13] P. Kushwaha, A.C. Gupta, P.J. Wiita, H. Gaur, E.M. de Gouveia Dal Pino, J. Bhagwan et al., *Multiwavelength temporal and spectral variability of the blazar OJ 287 during and after the 2015 December flare: a major accretion disc contribution*, **473** (2018) 1145 [1709.04957].

[14] J.C. Rodríguez-Ramírez, P. Kushwaha, E.M. de Gouveia Dal Pino and R. Santos-Lima, *A hadronic emission model for black hole-disc impacts in the blazar OJ 287*, **498** (2020) 5424 [2005.01276].

[15] S. Komossa, D. Grupe, M.L. Parker, M.J. Valtonen, J.L. Gómez, A. Gopakumar et al., *The 2020 April-June super-outburst of OJ 287 and its long-term multiwavelength light curve with Swift: binary supermassive black hole and jet activity*, **498** (2020) L35 [2008.01826].

[16] A. Agarwal, B. Mihov, I. Andruchow, S.A. Cellone, G.C. Anupama, V. Agrawal et al., *Multi-band behaviour of the TeV blazar PG 1553+113 in optical range on diverse timescales. Flux and spectral variations*, **645** (2021) A137 [2011.04074].

[17] A. Agarwal, S.A. Cellone, I. Andruchow, L. Mammana, M. Singh, G.C. Anupama et al., *Multiband optical variability of 3C 279 on diverse time-scales*, **488** (2019) 4093 [1908.01465].

[18] R. Prince, A. Agarwal, N. Gupta, P. Majumdar, B. Czerny, S.A. Cellone et al., *Multiwavelength analysis and modeling of OJ 287 during 2017-2020*, **654** (2021) A38 [2105.04028].

[19] Y.H. Zhang, A. Celotti, A. Treves, L. Chiappetti, G. Ghisellini, L. Maraschi et al., *Rapid X-Ray Variability of the BL Lacertae Object PKS 2155-304*, **527** (1999) 719 [astro-ph/9907325].

[20] R. Prince, G. Raman, J. Hahn, N. Gupta and P. Majumdar, *Fermi-large area telescope observations of the brightest gamma-ray flare ever detected from CTA 102*, *The Astrophysical Journal* **866** (2018) 16.

[21] J.R. Mattox, D.L. Bertsch, J. Chiang, B.L. Dingus, S.W. Digel, J.A. Esposito et al., *The Likelihood Analysis of EGRET Data*, **461** (1996) 396.

[22] H.T. Liu and J.M. Bai, *Absorption of 10-200 GeV Gamma Rays by Radiation from Broad-Line Regions in Blazars*, **653** (2006) 1089 [0807.3135].

[23] M.J. Valtonen, S. Zola, S. Ciprini, A. Gopakumar, K. Matsumoto, K. Sadakane et al., *Primary Black Hole Spin in OJ 287 as Determined by the General Relativity Centenary Flare*, **819** (2016) L37 [1603.04171].

[24] S. Laine, L. Dey, M. Valtonen, A. Gopakumar, S. Zola, S. Komossa et al., *Spitzer Observations of the Predicted Eddington Flare from Blazar OJ 287*, **894** (2020) L1 [2004.13392].

[25] H.J. Lehto and M.J. Valtonen, *OJ 287 Outburst Structure and a Binary Black Hole Model*, **460** (1996) 207.

PoS(Gamma2022)179